

## Design of semi-submersible offshore power generation platform based on green energy utilization

Qingyang Chen<sup>1, †</sup>, Chen Liang<sup>2, †</sup>, Zhihao Wang<sup>3, †</sup> and Baoxu Zhang<sup>4, \*, †</sup>

<sup>1</sup>Department of Civil and Environmental Engineering, The Hong Kong Polytechnic University, Hung Hom, Kowloon, Hong Kong

<sup>2</sup>Department of Civil Engineering, Qingdao University of Technology, Qingdao, Shandong, China

<sup>3</sup>Chang'an Dublin International College of Transportation, Chang'an University, Xi'an, Shaanxi, China

<sup>4</sup>College of Civil Engineering, Fuzhou University, Fuzhou, Fujian, China

\*Corresponding author: 051901240@fzu.edu.cn

†These authors contributed equally.

**Abstract.** In recent years, wind energy is receiving increasing attention as a non-polluting, renewable, efficient and clean marine green energy source, and countries around the world are already stepping up their development and utilization of wind energy. This paper discusses the design parameters and data analysis of a feasible semi-submersible offshore wind power platform based on the integrated use of green energy for economic purposes under given hydrographic conditions. The design parameters of the power platform include the combination of a circular floating platform, columns, 4.2 MW turbine, floats, and trusses and their respective dimensions, while the data analysis emphasizes the initial stability analysis by verifying the distance between the steady center floats, the wave load calculation by calculating the magnitude of the Morrison force on the floats in waves, the wind load calculation by using static theory to deal with the structural forces at constant wind speed and the cost calculation by adding up the costs of various items. The results of the data analysis show that the designed platform has good initial stability, can withstand wave and wind loads under the design conditions, and that the cost of the materials used in the structure is reasonable. The draft design presented in this paper is expected to provide an alternative design for upgrading existing offshore power generation platforms, achieving a combined use of solar and wind energy, and reducing the cost of building semi-submersible offshore power generation platforms.

**Keywords:** ocean energy, floating platform, wind power, solar power, structural response analysis.

### 1. Introduction

Ocean energy, as defined by the International Renewable Energy Agency (IRENA), is primarily a way of generating electricity using the ocean's conditions (movement, its own physical and chemical properties). Ocean green energy has great potential, according to the IRENA, the combined power generation potential of all ocean energy technologies is 45,000-130,000 TWh, which means that ocean energy could meet more than twice the current global electricity demand, and is therefore considered a reliable, sustainable, predictable, and cost-competitive source of energy, despite its higher energy density and the difficulty of harnessing it compared to other energy sources. Among the various renewable energy sources, wind energy is gaining importance as a non-polluting, renewable, efficient, and clean new energy source. China's rich offshore wind resource reserves, according to the results of previous wind resource surveys, indicate that China's offshore wind power development potential is about 200 million kW at 5-25 m water depth and 50 m height, and about 500 million kW at 5-50 m water depth and 70 m height. The rich resource potential, as well as the good consumption capacity, determines that China's offshore wind power is promising, Fig. 1 accurately demonstrates that in 2020 China's wind turbine development has had a huge impact on the world market.

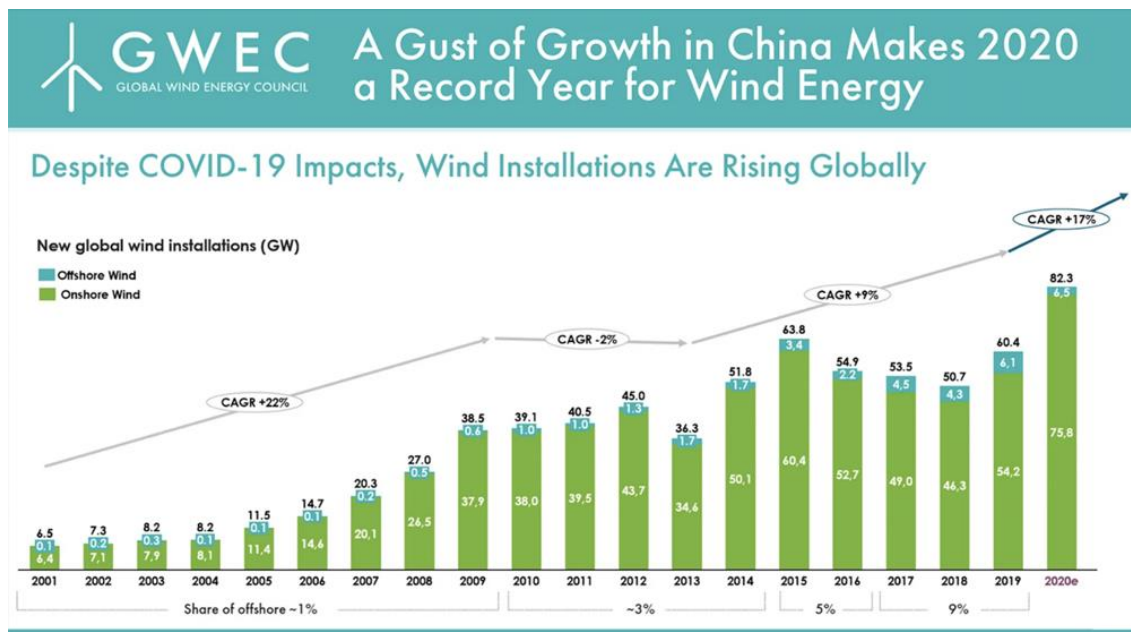


**Fig. 1** GWEC A Gust of Growth in China Makes 2020 a Record Year for Wind Energy [1]

However, marine energy technology development currently faces many risks and uncertainties, such as the difficulty of development, low energy density, partial energy instability, harsh environmental loading conditions, and complex seabed conditions. To solve these problems, the current development trend mainly emphasizes the realization of stable power generation from core technology and equipment and the comprehensive use of marine energy development, so to enhance the overall development level of marine energy and form the initial scale of engineering applications. At this stage, although there have been many diverse patented designs for offshore power platforms, such as the Fukushima-FORWARD Floating Project in Japan by Mitsui Engineering & Shipbuilding, WINFLO in France and Song Zhaobo [2, 3]. However, most of these offshore platform designs are still limited to the single use of offshore wind energy and are not able to consider a comprehensive range of marine green energy sources.

This paper will explore the complete design and modeling of a feasible semi-submersible offshore wind and solar power platform based on the integrated use of green energy under given hydrographic conditions, and evaluate the reasonableness of the designed platform in three dimensions: ballast design and initial stability verification, wave and wind load calculation and cost estimation, so that the structure can be adapted to the deep sea environment while meeting the requirements of low carbon emissions and construction costs, and achieving the scaled-up, economic and effective integrated use of green energy.

## 2. Method

### 2.1. Design Philosophy

This paper discusses the creative design of a floating offshore power platform in a known sea area with a maximum water depth of 50 m, a 50-year return period, a maximum wave height of 8 m, and a corresponding period of 10 s. Following an analysis of the difficulty and feasibility of the calculations, the draft presented in this paper chooses a simpler conventional wind tower form and a circular floating platform for further design calculations, and this combination results in a floating offshore structure design that meets the given hydrographic conditions. A semi-submersible structure with multiple columns is chosen to meet the dual requirements of stability and 50m water depth. Compared with other types of platforms, the semi-submersible platform is applicable to a wider range of water depths and more convenient for construction and installation [4]. The structure consists of a circular floating platform, seven columns, three wind towers (each with a 120-degree line of sight to

the center of the circle), floats, and trusses. The design will combine the understanding of wind and solar energy development to maximize the use of offshore green energy, with the final structure having a total power of not less than 10 MW for wind power and 2 MW for photovoltaic power.

## 2.2. Structural Stability

### 2.2.1 Basic concept of initial stability

The ability of the ship to return to the original equilibrium position on its own after the external force is removed is called ship stability [5]. According to the size of the tilt angle, the stability can be divided into small tilt stability (tilt angle less than  $10^\circ\sim 15^\circ$ ) and large tilt stability (tilt angle more than  $10^\circ\sim 15^\circ$ ), and the design part of this paper mainly considers the initial stability. For floating structures at sea, it is the most basic and important step to check whether the stability meets the requirements, because it is directly related to whether the structure can work stably at sea without overturning and other phenomena.

### 2.2.2 Initial stability calculation method

In the calculation of the initial stability, the main verification is divided into two parts - whether the center of gravity of the floating platform is lower than the floating center, whether the center of gravity of the overall structure is lower than the floating center (SPAR) or whether the center of gravity is lower than the stable center (semi-submersible platform); and the two parts of the verification idea is the same, both require the iterative process of ballast design and weight determination, calculation of the structural center of gravity, floating center, drainage, and total weight, and height calculation of the center of gravity and floating center until the data that meet the conditions are obtained that stops the iteration. Its calculation method and equation mainly use the stability calculation equation under a small inclination angle.

Fig. 2 represents the case of a structure tilted at a small angle ( $\phi$ ) under the action of external forces, assuming an equal volume tilt, the intersection of the waterline surface through the original waterline from the center (also called the floating center), WL is the initial waterline,  $W_1 L_1$  is the new waterline, G is the center of gravity of the overall structure, its floating center moves from B to  $B_1$ , the moving trajectory of the floating center  $BB_1$  is called the floating center curve [5]. The center of curvature of the buoyancy curve (i.e., the center of the arc) is called the stable center of the ship, which is expressed by the symbol "M". The stable center M can be regarded as the intersection of the buoyancy lines before and after the small inclination of the ship. The center of stability M can be considered as a fixed point. If it is required to maintain a stable state,  $BB_1$  must be larger than the projection of  $|BG|$  on  $|BB_1|$ , such as  $|GM| > 0$ , in order for the buoyancy force and gravity to produce a restoring moment to maintain its equilibrium.

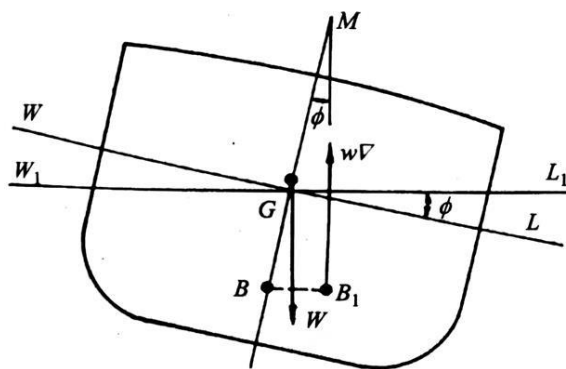


**Fig. 2** Floating center movement diagram

According to Shanghai Jiao Tong Press "Ship Statics", the formula of the initial stability high (GM) can be deduced (equation (1)-(2)), where  $g_1$  refers to the position of the center of gravity of the inlet volume,  $v_1$  is the inlet volume, and  $V$  is the total discharge volume, O is the focal point of water

surface lines, and all of which can be obtained by integrating its value [6]. Therefore, the final index of the outgoing stability verification is to satisfy  $|GM| > 0$ .

$$|BB_1| = 2 |g_1O| v_1 / \nabla \quad (1)$$

$$|GM| = |BM| - |BG| = |BB_1| / \phi - |BG| \quad (2)$$

### 2.3. Wave Load and Wind Load

#### 2.3.1 Wave load calculation method

Wave load, as the maximum load on the offshore building, has a great influence on the stability, safety, and applicability of the structure. The wave force on the structure is related to the water depth, wave height, and period of the sea, as well as the structural form and arrangement of the structure and the shape of the interface. Here, we only discuss the wave force on the cylindrical members arranged in the vertical direction, which is most common in marine engineering. For the floating part of this offshore platform, its diameter wavelength ratio was 0.08, then it is assumed that the existence of small members does not affect the wave propagation motion, and the Morrison force method is used to calculate the wave force load, so the wave force can be superimposed by the drag force and inertia force [7].

#### 2.3.2 Wind load calculation method

The wind speed in nature is not constant and has both long-period and short-period components. There is a pulsating variation of wind speed around its average value, i.e., there are spectral characteristics. The structure will vibrate under the action of wind, producing deformation and causing fatigue damage to the structure. From this design engineering practical purpose, according to the average wind for calculation and analysis, the role of the static nature, so that the use of static theory to approximate the action of the wind load average wind, that is, constant wind speed under the force of the structure is equivalent to the static force, and the greater the wind speed, the greater the action of the pressure on the structure.

### 2.4. Overall Cost Estimation

Generally, the cost of an offshore wind farm consists of the following components: equipment cost, construction and installation costs, other costs, and interest, while the cost differences between offshore wind power and onshore wind power are mainly in equipment costs, installation costs, and operation and maintenance costs. According to the feasibility of the offshore wind power project cycle and overall calculation, the cost analysis in this paper mainly considers the investment costs during the development and construction phase of the project, such as equipment costs, construction and installation costs, and other costs, and uses the current average level of offshore wind power project costs in China as the basis for the corresponding cumulative calculation.

## 3. Wind Power Platform Design and Initial Stability Test

### 3.1. Appearance design concept diagram and parameters

Fig. 3 shows the detailed diagram of the lower part of the floating platform, specifically showing the truss connection form, the floating tube setting method, and the relative position details; Fig. 4 shows the specific detail diagram of the upper part of the floating platform combined with the fan, including the fan setting position and the fan form details.

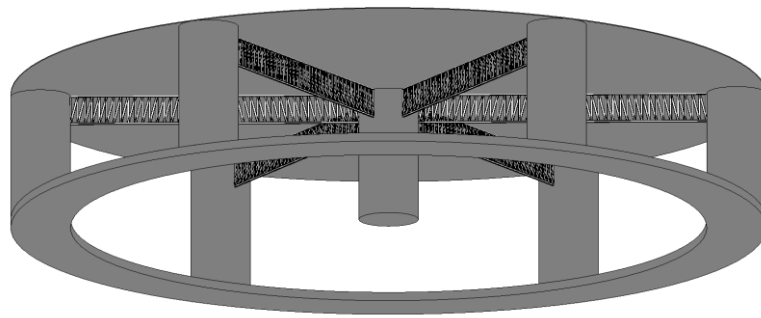


**Fig. 3** Reference diagram of final design ideas (floating platform)

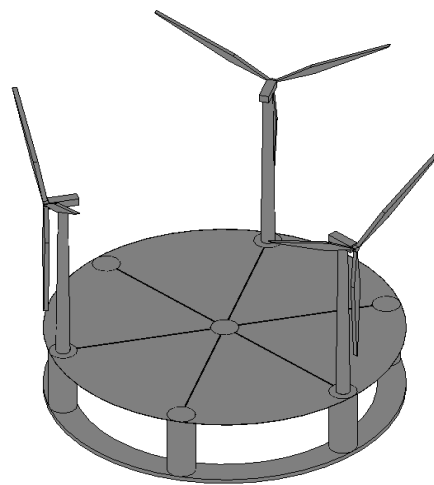


**Fig. 4** Reference diagram of final design ideas (complete platform)

The specific basic parameters such as dimensions and masses chosen for each component of the conceptual design of the project are given in Table 1-4. Table 1 and Table 2 are the conceptual design parameters of the wind tower and the basic parameters of the materials used, Table 3 shows the specific information of the photovoltaic panels utilized for solar power generation, Table 4 shows the design parameters of the semi-submersible platform. Fig. 5 and Fig. 6 are the modeling schematics of the wind tower and floating platform structures, respectively.

**Table 1.** Wind power tower design parameters t

Parameters	Numerical value
Rotor radius (m)	57.2
Rotor mass (kg)	70,000
Motor mass (with nacelle) (kg)	100000
Diameter of tower carrier surface1 (m)	6
The thickness of the tower carrier surface1 (mm)	30
Diameter of tower carrier surface2 (m)	4
The thickness of tower barrel carrier surface2 (mm)	20
Total mass of tower (kg)	200000
Wind power tower column height (m)	80
Wind power tower power (MW)/pc	4.2

**Table 2.** Fan material parameters

Parameters	Numerical value
Modulus of elasticity (GPa)	206
Shear modulus (GPa)	154.5
Yield strength (MPa)	345
Density (kg/m <sup>3</sup> )	7.85
Poisson's ratio	0.5

**Table 3.** Photovoltaic panel design parameter

Parameters	Numerical value
Support truss weight per square meter (kg/m <sup>2</sup> )	0.2
Photovoltaic panel weight per square meter (kg/m <sup>2</sup> )	13
Photovoltaic panel area (m <sup>2</sup> )	10368
Total rated power (MW)	20736
Total mass(kg)	134784
Height of center of gravity (m)	1

**Table 4.** Semi-submersible platform design parameters

Parameters	Numerical value
Platform mass (kg)	2024829
Platform center of gravity position (m)	9.404
Platform radius (m)	70
Float width (m)	12
Float height (m)	2
Column diameter (m)	12
Column height (m)	30
Column and float thickness (m)	0.02
Ballast mass(kg)	21440000
Ballast center of gravity position (m)	0.83

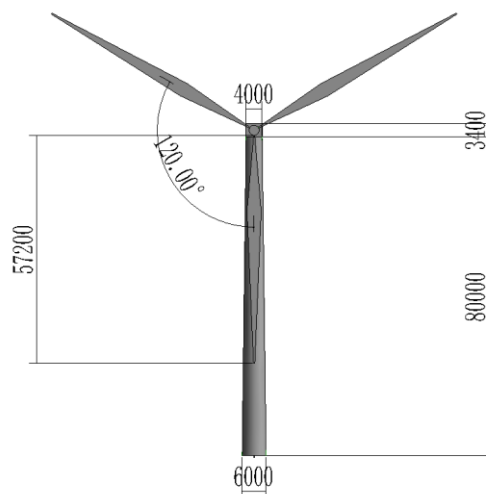


**Fig. 5** Schematic diagram of wind turbine modeling

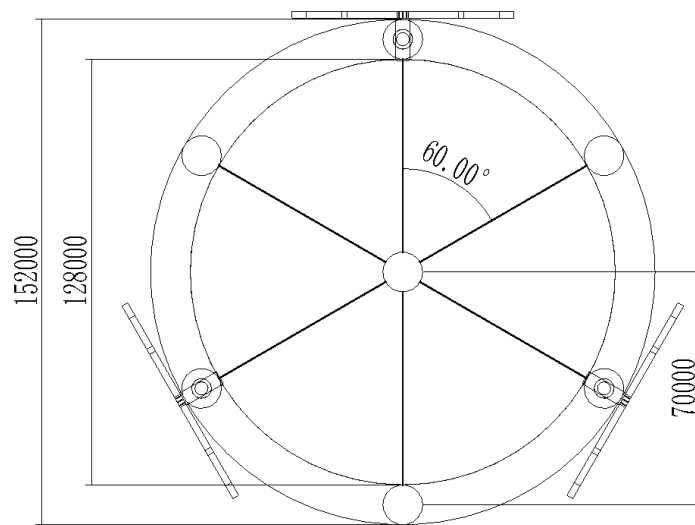


**Fig. 6** Schematic diagram of floating platform modeling

### 3.2. Ballast design data and initial stability calculations

#### 3.2.1 Basic concept of initial stability

The following tables illustrate specific information on platform drainage (Table 5), give information on the center of gravity and mass of the superstructure (Tables 6-7), and specific information on ballast (Table 8).

**Table 5.** Wind power platform floating center and drainage volume parameters

Parameters	Numerical value
Design draught (m)	26
Drainage volume (m <sup>3</sup> )	26841.77
Discharge volume (kg)	27647023.10
Seawater density (kg/m <sup>3</sup> )	1030
Float tube floating center height (m)	1
Column floating center height (m)	14
Floating center height (m)	8.89
Drainage volume of float tube (m <sup>3</sup> )	10555.75
Drainage volume of column (m <sup>3</sup> )	16286.01

**Table 6.** Cover design parameters

Parameters	Numerical value
Cover volume (m <sup>3</sup> )	692.72
Discharge volume (kg)	5437852
Height of center of gravity of cover (m)	32.09

**Table 7.** Fan design parameters table

Parameter Name	Numerical value
Fan mass (kg) (3 units)	930000
Center of gravity height (m)	115.63
Tower mass (kg) (3 units)	600000
Center of gravity height (m)	69.11
Total mass (kg)	1530000
Total center of gravity height (m)	97.38

**Table 8.** Table of ballasted concrete design parameter

Parameter Name	Numerical value
Density kg (m <sup>3</sup> )	2450
Height (m)	1.66
Volume (m <sup>3</sup> )	8751
Mass (kg)	21440000

### 3.2.2 Initial stability test

The design draught of this structure is 26 m, the calculated drainage volume is 29556 m<sup>3</sup>, the origin of the coordinate system is taken in the lowermost plane of the whole structure, the height of the floating center under this coordinate system is about 8.89 m, the buoyancy generated can carry about 30000 t of mass, the mass of the platform is 2024829 kg, the height of its center of gravity is 9.404 m, the mass of the circular cover on the upper part of the platform is 543782 kg. The total mass of the wind turbine and photovoltaic solar panel on the platform is about 1530000 kg, and the height of the center of gravity is 97.83 m. The ballast concrete is all in the lowermost circular float, the height of the concrete is 1.7 m, and the mass is 21440000 kg. The height of the center of gravity of the whole structure is calculated to be about 14 m, and the height of the floating center is about 8.89 m. Using BIM modeling software assistance, can be derived from the drainage volume and length of  $|g_1O|$ , which will be brought into the initial stability test formula that can be concluded that the initial stability height is around 20.17 m, which meets the stability requirements. However, it should be noted that this structure only considers its stability at work and makes the assumption of a small inclination angle, and there may be some errors for its stability at towing, and some approximations are made during data processing, and the results obtained are approximate solutions that are closer to the real situation rather than analytical solutions.

### 3.3. Load calculation

#### 3.3.1 Wave load

The following are all the calculation processes involved in the wave loads on individual floats and the results. The wave number and wave length were calculated according to equation (3).

$$\Delta = \frac{k}{D} \quad (3)$$

where,  $\Delta$  is the relative roughness,  $k$  is the surface roughness coefficient, and  $D$  is the float diameter. The relative roughness is  $4.167 \times 10^{-7}$ .

$$Re = \frac{u_{\max}}{\nu} \quad (4)$$

where,  $u_{\max}$  is the maximum water quality point velocity which is 1.2566 meters per second,  $\nu$  is the coefficient of roughness, and  $Re$  is the Reynolds coefficient and equal to  $1.1528 \times 10^7$  according to equation (4).

$$K_c = \frac{\pi H}{D} \quad (5)$$

where,  $K_c$  denotes the Keulegan-Carpenter number, which is 2.0943 and less than 3. According to the Reynolds coefficient and relative roughness, drag force coefficient  $C_D$  can be obtained from Figure 7, the drag force coefficient  $C_D$  is 1.0,  $C_A$  is 1, so the  $C_M$  is 2.0

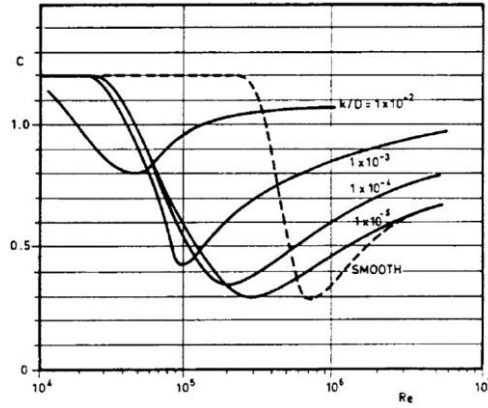


**Fig. 7** The drag force coefficient

The maximum wave height is 8 m and maximum period is 10 s. According to the dispersion equation (equation (6)), the wave number was calculated as  $0.0415 \text{ m}^{-1}$  and wavelength was calculated as 151.402 m.

$$\omega^2 = gk \tanh(kd) \tag{6}$$

where,  $\omega = 2\pi / T$  and  $g = 9.8 \text{ m/s}^2$ .

$$u = \frac{\pi H_{\max}}{T_{\max}} \cdot \frac{\cosh\left(ks \frac{d}{d+\eta}\right)}{\sinh kd} \cdot \cos \alpha = 1.5689 \cosh\left(ks \frac{d}{d+\eta}\right) \cdot \cos \alpha \tag{7}$$

$$a = \frac{2\pi^2 H_{\max}}{T_{\max}} \cdot \frac{\cosh\left(ks \frac{d}{d+\eta}\right)}{\sinh kd} \cdot \sin \alpha = 0.9858 \cosh\left(ks \frac{d}{d+\eta}\right) \cdot \sin \alpha \tag{8}$$

Equation (7) and (8) represents the wave velocity and acceleration, where  $u$  is the wave velocity,  $a$  is the wave acceleration,  $k$  is the wave number,  $s$  is the water surface height,  $d$  is the water depth,  $n$  is the wave amplitude, and  $\alpha$  is the wave phase angle. Wave force can be determined by the sum of inertia force and drag force according to equation (9). Formula (10) is the amplitude of the wave. Equation (11) represents the wave force at every point of the float bow, the result is  $2.22968 \times 10^5 \times \cosh\left(\frac{2.075s}{50+4 \cos \alpha}\right) \sin \alpha + 1.4768 \times 10^4 \times \left[\cosh\left(\frac{2.075s}{50+4 \cos \alpha}\right) \cos \alpha\right]^2$ .

$$f = f_I + f_D = C_M A_I a + C_D A_D u |u| \tag{9}$$

where,  $A_I = \rho_w \frac{\pi D^2}{4} = 1.1309 \times 10^5 \text{ kg/m}$  and  $A_D = \frac{1}{2} \rho D = 6000 \text{ kg/m}^2$ ,  $A_I$  and  $A_D$  are the area of inertia force, area of drag force respectively.

$$\eta = \frac{H_{\max}}{2} \cos \alpha = 4 \cos \alpha \tag{10}$$

$$f = C_M A_I a + C_D A_D u |u| \tag{11}$$

The draft depth is 26m and the seawater depth is 50m, and the Morrison force is obtained by integrating over the force interval. Following are the results in equation (12) and equation (13).

$$\text{For } \alpha \in \left[0, \frac{\pi}{2}\right] \cup \left[\frac{3\pi}{2}, 2\pi\right]$$

$$F = \int_{24}^{50+4 \cos \alpha} 2.22968 \times 10^5 \times \cosh\left(\frac{2.075s}{50+4 \cos \alpha}\right) \sin \alpha + 1.4768 \times 10^4 \times \left[\cosh\left(\frac{2.075s}{50+4 \cos \alpha}\right) \cos \alpha\right]^2 ds \tag{12}$$

$$For \alpha \in \left[ \frac{\pi}{2}, \frac{3\pi}{2} \right]$$

$$F = \int_{24}^{50+4\cos\alpha} 2.22968 \times 10^5 \times \cosh\left(\frac{2.075s}{50+4\cos\alpha}\right) \sin \alpha - 1.4768 \times 10^4 \times \left[ \cosh\left(\frac{2.075s}{50+4\cos\alpha}\right) \cos \alpha \right]^2 ds \quad (13)$$

Curve representing relationship between the wave force F and the wave phase angle  $\alpha$  can be obtained from Fig. 8, which is created by MATLAB.

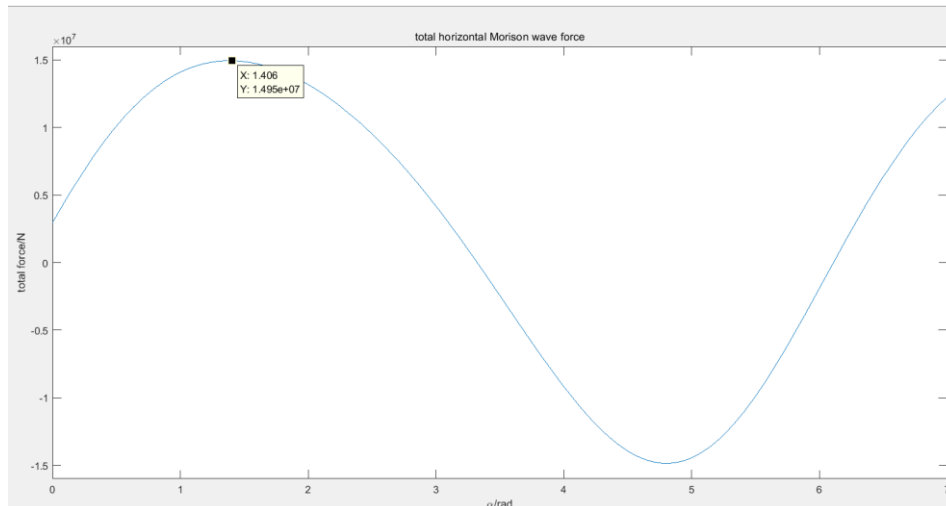


**Fig. 8** Relationship between the wave force and the wave phase angle

As can be seen from the figure, the maximum Morison force on a single float is  $1.495 \times 10^7$  N when the wave phase angle is 1.406 rad. According to Giuseppe Giorgi et al., their results show that Wheeler stretching provides good accuracy and complexity trade-offs for wave force calculations for operation on offshore platforms [8].

### 3.3.2 Wind load

This design uses the wind load calculation Equation provided in the ABS Code (2014), as shown in equation (14).

$$F = f \cdot v_k^2 \cdot C_h \cdot C_s \cdot A \quad (14)$$

where, f is 0.611,  $C_h$  is height factor,  $C_s$  is shape factor, A is the wind area of the member,  $v_k$  is the design wind speed at a height of 15.3m above the hydrostatic surface for 1 min.

The design is a fifty-year sea state, according to the latest typhoon news released by the Central Weather Bureau on August 25, 2022 - typhoon "Ma On" for reference, the maximum wind speed near its center 33 m/s, for conservative calculation of wind load to take the design wind speed 35 m/s. Check table 9 to take the fan height factor  $C_{h1}$  is 1.43, PV panel height factor  $C_{h2}$  is 1.00. Check Table 10 to take the fan shape factor  $C_{s1}$  is 1.5, PV panel shape factor  $C_{s2}$  is 1.0

**Table 9.** Height coefficients  $C_h$  [9].

Height above sea level (h/m)	Height factor $C_h$
0-15.3	1.00
15.3-30.5	1.10
30.5-46.0	1.20
46.0-61.0	1.30
61.0-76.0	1.37
76.0-91.5	1.43
91.5-106.5	1.48
106.5 - 122.0	1.52
122.0-137.0	1.56

**Table 10.** Shape coefficients  $C_s$  [9].

Shape	Shape factor $C_s$
Spherical	0.4
Cylindrical (all sizes)	0.5
Housing plate	1.0
Deck Room	1.0
Isolated structures (cranes, angles, channels, beams, etc.)	1.5
Steel cable	1.2
Below deck area (smooth surface)	1.0
Below deck area (exposed beams and joists)	1.3
Small components	1.4
Drilling rigs	1.25

Calculate the wind area of a single fan according to model  $A_1$  is 400 m<sup>2</sup>, All solar panels are subjected to wind area  $A_2$  is 5184 m<sup>2</sup>. Calculate single fan wind load is 642191.55 N, and all solar photovoltaic panels wind is 3880094.4 N. So unit wind loads are 1605.478875 N/m<sup>2</sup> and 748.475 N/m<sup>2</sup>. The calculated wind load on the structure meets the ABS code requirements and the strength is up to standard.

#### 4. Cost estimation

The detailed procedure for cost estimation works contains three main parts -- equipment cost calculation, equipment cost per kilowatt calculation and total cost per kilowatt calculation. Table 11 shows details of five equipment variables gathered in the design and their variations while equation (15) illustrates the measure of equipment cost summation. For the calculation of cost of equipment per kilowatt, as shown in equation (16), the total equipment cost should be divided by the total working power of the equipment. Table 12 delineates the outcome and parameters used for this calculation. The last part in cost estimation is the summation of costs per kilowatt, the measure for adding up the three aspects is expressed by equation (17), Table 13 summarizes the details for different cost parameters and the result of cost estimation.

$$\text{Total Equipment Cost} = \text{Equipment Cost Per Unit} \times \text{Number of Units} \quad (15)$$

$$\text{Cost of Equipment Per Kilowatt} = \frac{\text{Total Equipment Cost}}{\text{Total Equipment Power (MW)} \times 1000} \quad (16)$$

$$\text{Total Cost Per Kilowatt} = \text{Cost of Equipment Per Kilowatt} + \text{Cost of Construction \& Installation Per Kilowatt} + \text{Other costs Per Kilowatt} \quad (17)$$

**Table 11.** Equipment cost statistics

Equipment name	Unit cost (¥/unit)	Total construction cost (¥)
Wind turbine (Vestas V136-4.2MW)	24533795.62	73601386.86
Photovoltaic panels	900	9331200
Floating platform	4600	9314213.4
Ballasted concrete	550	4813050
Covers	6300	34258467.6

**Table 12.** Cost statistics for per kilowatt of equipment

Overall equipment cost (¥)	Total power of equipment (MW)	Cost of equipment per kilowatt (¥)
131318317.9	12.6	10422.08872

**Table 13.** Total cost per kilowatt statistics

Equipment cost per kilowatt (¥)	Construction and safety costs per kW (offshore booster station, wind turbine, etc.) (¥)	Other costs per kW (land use, construction, and management, submarine cable, etc.) (¥)	Total construction cost per kilowatt (¥)
10422.08872	25000	10000	45322.09

The construction cost of the scenic power equipment used in this design is estimated to be approximately ¥10,422 per kilowatt and the overall offshore power platform construction cost is approximately ¥45,322 per kilowatt. Although the design in this paper adds the cost of photovoltaic panels, the construction cost of the wind and solar equipment is still relatively economical compared to the US\$1966 per kilowatt for the Aqua Ventus 12 MW turbine in 2018 as indicated in Musial et al [10]. The total cost of constructing the offshore power platform is the total cost of building the offshore platform is higher than the US\$3739 per kilowatt mentioned in the paper, due to the higher requirements of operation and maintenance costs for combined utilization of solar and wind energy in the design, and the fact that the cost of building and installing three split turbines is much higher than the cost of one 12 MW turbine. Overall, the design of this paper makes every effort to integrate wind and solar energy while minimizing non-essential construction costs, and the higher cost relative to conventional semi-submersible offshore platforms can be considered a ‘meaningful sunk cost.

## 5. Conclusion

At present, the development of wind power has become the core content of promoting energy transformation in many countries and dealing with climate change, finding ways for comprehensive utilization of offshore wind power has thus become a common proposition for all countries in recent years. This paper proposes a complete parametric design and modeling of a semi-submersible offshore platform, using a combination of three 4.2 MW wind turbines, 10368 m<sup>2</sup> photovoltaic panels, 5437852 kg cover plates, and 21440000 kg concrete ballast on a structure radius of 70m and a buoy width of 12 m floating platform. The initial stability evaluation of the overall structure after ballast is 20.17 m>0; the maximum value of Morrison force on a single buoy is 1.495×10<sup>7</sup> N; the wind turbine and photovoltaic panels experience wind loads of 1605.478875 N/m<sup>2</sup> and 748.475 N/m<sup>2</sup> respectively when subject to the design wind speed of 35 m/s; the equipment and total cost per kilowatt is about ¥ 10422 and ¥ 45322. This design scheme can be considered as reasonable in all four aspects including design idea, initial stability, wind and wave loads, and cost estimation. In the future, other researchers should focus more on the consideration of static stability curves and random wave loads, so that this structure can become a more comprehensive design that in line with realistic conditions.

## References

- [1] Pek, A. (2021, January 21). A gust of growth in China makes 2020 a record year for wind energy. Global Wind Energy Council. <https://gwec.net/a-gust-of-growth-in-china-makes-2020-a-record-year-for-wind-energy/>.
- [2] Leimeister<sup>1</sup>, M., Kolios<sup>1</sup>, A., & Collu<sup>1</sup>, M. (2018, October 1). IOPscience. Journal of Physics: Conference Series. <https://iopscience.iop.org/article/10.1088/1742-6596/1104/1/012007>
- [3] Song Zhaobo, Shi Wei, Zhang Lixian, Li Li, Li Xin, Wang Bin. (2021) Design and stability of large semi-submersible floating wind turbine platform[J]. Journal of Ocean University of China (Natural Science Edition),51(11):102-109.
- [4] Cao Q., Xiao L., Guo X., et al. (2020). Second-order responses of a conceptual semi-submersible 10 MW wind turbine using full quadratic transfer functions. Renewable Energy, 153.
- [5] Sheng, Z.B. (2017) Principles of ships: upper volume. Shanghai Jiaotong University Press. Shanghai.
- [6] Zhang Baoji. (2016) Ship statics [M]. Shanghai Jiaotong University Press. Shanghai.
- [7] Wang Shuqing, Liang B.C. (2013). China Ocean University Press. Qingdao.

- [8] Journal of Ocean Engineering and Marine Energy Received: 7 September 2017 / Accepted: 18 December 2017 © Springer International Publishing AG, part of Springer Nature 2017 of Springer Nature 2017.
- [9] American Bureau of Shipping (2005) Commentary on the ABS rules for building and classing mobile offshore. [https://ww2.eagle.org/content/dam/eagle/rules-and-guides/archives/offshore/6\\_modu2001/modu\\_commentary-combined\\_01-dec-04.pdf](https://ww2.eagle.org/content/dam/eagle/rules-and-guides/archives/offshore/6_modu2001/modu_commentary-combined_01-dec-04.pdf).
- [10] Musial, W., Beiter, P., & Nunemaker, J. (2020). Cost of floating offshore wind energy using New England Aqua Ventus concrete semisubmersible technology. <https://doi.org/10.2172/1593700>